Electrochemical Quartz Crystal Microbalance Studies of Electron Addition at Nanocrystalline Tin Oxide/Water and Zinc Oxide/Water Interfaces: Evidence for Band-Edge-Determining Proton Uptake

Buford I. Lemon and Joseph T. Hupp*

Department of Chemistry, Northwestern University, Evanston, Illinois 60208

Received: June 17, 1996; In Final Form: January 20, 1997[⊗]

Electrochemical quartz crystal microbalance (EQCM) measurements provide compelling evidence for charge-compensating cation uptake by nanocrystalline SnO_2 and ZnO electrodes during electron addition. Comparative light water/heavy water measurements establish that the adsorbed or intercalated ions are protons or deuterons. Additional studies as a function of pH implicate water, rather than hydronium ions, as the proton source. The new results, when combined with previous results for titanium dioxide in nonaqueous electrolytes, suggest that charge-compensating cation intercalation is a general mode of reactivity for metal oxide semiconductors. Finally, the new observations raise significant fundamental questions concerning (1) chemical control of band energetics, (2) possible band-edge-unpinning phenomena, and (3) relationships between band edge energies and driving forces for isolated electron transfer reactions.

Introduction

N-type nanocrystalline semiconductors based on metal oxide materials have attracted considerable attention from condensed-phase chemists because of their unusual electrochemical[1−3] and photochemical properties[4] and the convenience with which they can be assembled in high-area thin-film[5] or colloidal form.[6] Valence band properties[7] have been exploited in photocatalytic waste remediation,[8] photochemical synthesis[9] and photoelectrochemical energy conversion schemes.[10] Conduction band properties,[7] on the other hand, have been exploited in dye sensitization (electrochemical photovoltaic and photographic) schemes[11] and in fundamental studies of fast interfacial charge transfer processes.[12] N-type metal oxide semiconductors also are of intrinsic interest because of their typically diode-like interfacial electrochemical behavior: In the absence of mid-gap surface states, current flow from a dark semiconductor electrode to a redox-active solution species is usually small except under conditions where conduction band electrons have become energetically accessible at the electrode/solution interface.[13,14]

For N-type semiconductors, including metal oxides, reactive electrons[14] can be supplied electrochemically by externally biasing at potentials more negative than the conduction band edge E_{CB}. They also can be supplied photochemically—either by bandgap excitation and electron/hole pair generation, followed by hole scavenging, or by dye injection. Several recent studies of metal oxide semiconductors in nanocrystalline form have shown that electron addition via both schemes can be observed optically and that the potential for the onset of addition changes, as expected, with environment-induced changes in E_{CB} (most notably, Nernstian shifts in E_{CB} with solution pH).[1a,e,3,15]

We recently showed that electron addition to the nanocrystalline titanium dioxide/nonaqueous electrolyte interface is accompanied quantitatively by the intercalation of charge-compensating alkali metal cations or by adsorption of larger *molecular* cations.[16,17] Here we report that the phenomenon is more general: Electron addition at nanocrystalline zinc oxide/water and tin oxide/water interfaces is similarly accompanied by uptake of charge-compensating cations. Electrochemical quartz crystal microbalance (EQCM) measurements in light and heavy water establish that the adsorbed or intercalated ions are protons or deuterons, while pH-dependent measurements indicate that the proton source is almost certainly water rather than hydronium ion. The new observations have interesting implications in terms of field effects (bulk electrodes), band edge energetics, and electron transfer mechanisms.

Experimental Section

Ethanolic ZnO sols were prepared by a method similar to that of Spanhel and Anderson[18] as modified by Hoyer et al.[3b] This method yields nanocrystalline semiconductor particles having diameters of roughly 5 nm. SnO_2 solutions (3−5 nm particle diameter) were purchased from Alfa as 15% solutions in water. To facilitate film formation from both sols, 1 drop of surfactant solution (Triton X-100, Aldrich) was added for each ml of solution. Solution/surfactant mixtures were then spin coated onto the keyhole-shaped gold electrode portions (A_e = 0.205 cm^2) of masked quartz crystals (5 MHz oscillators; ICM, Inc.), with 5 min of heating at 100 °C between each of several coatings. Following the final coating, films were heated for 1 h in air at 400 °C. Films were also prepared on transparent or semitransparent substrates (microscope slides, fluorine-doped tin oxide on glass (Thin-Films Research, Westford, MA) or indium-doped tin oxide on glass (ITO; PPG Industries)). These films yielded absorption spectra that were consistent with literature reports.[19]

EQCM measurements were performed largely as previously described[16] except that an in-house module written with Labview software (National Instruments Corp., Austin, Texas) was used for PC-based data collection and instrument control.

Electrolyte solutions consisted of appropriate buffers in either H_2O (Milli-Q water purification system) or D_2O (Aldrich, 99.9%). Buffering was achieved with sodium acetate/acetic acid (pH 4 and 5), sodium borate/hydrochloric acid (pH 8), or sodium borate with NaOH (pH 10). Electrochemical measurements were made with a PAR 273 potentiostat in a one-compartment cell containing a platinum wire counter electrode and a saturated (sodium) calomel reference electrode (ssce). All potentials are reported versus ssce.

[⊗] Abstract published in *Advance ACS Abstracts,* March 1, 1997.

S1089-5647(96)01780-4 CCC: $14.00

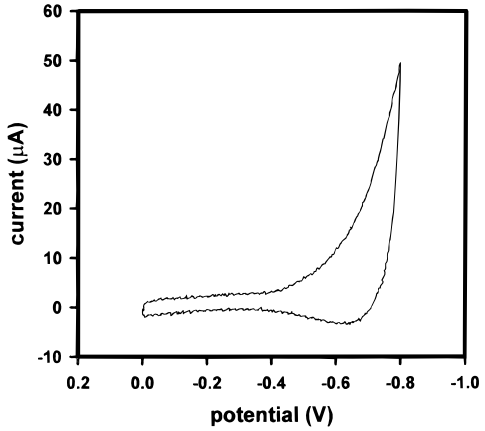

Figure 1. Cyclic voltammetry of a nanocrystalline tin oxide film at pH 10.

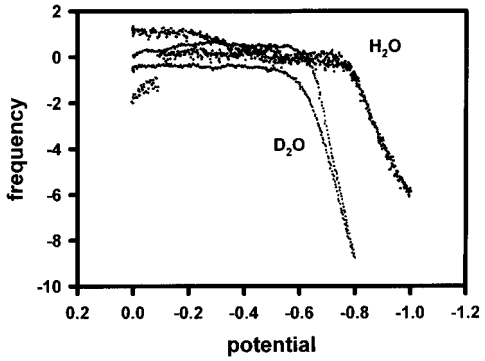

Figure 2. Oscillator frequency versus potential plot for nanocrystalline tin oxide illustrating mass uptake in H_2O and D_2O at potentials negative of E_{CB}. Scan rate = 50 mV/s.

Results

Tin Oxide. Nanocrystalline tin oxide was interrogated in thin-film form by electrochemical and quartz crystal microbalance methods. Figure 1 shows a voltammogram recorded at 50 mV/s in water buffered at pH 10. At potentials positive of −400 mV, the electrode is electronically insulating and current is absent. In an idealized description of the interface, at potentials negative of ca. −400 mV, the Fermi level exceeds E_{CB} (i.e., the applied potential is more negative than E_{CB}). The reversible addition of electrons is possible, as demonstrated by the passage of current. In principle, the process should yield symmetrical voltammograms. The deviations from symmetry in Figure 1 become more pronounced at lower sweep rates and in less thoroughly deoxygenated solutions. Presumably they are associated with additional current flow due to dissolved oxygen reduction and perhaps also solvent reduction.

Figure 2 shows the quartz crystal microbalance response from a tin oxide electrode under the same conditions as in the voltammetry experiment. The most notable feature is the sharp decrease in crystal oscillation frequency f corresponding to an increase in film mass, m, beginning at $E \approx E_{CB}$ (i.e., the potential where electrons begin to add to the film). From the Sauerbrey expression (eq 1),[20] the absolute change in electrode mass can be estimated from the frequency change.

$$\Delta f = (56.6 \text{ Hz cm}^2\, \mu\text{g}^{-1})\Delta m/A_e \qquad (1)$$

Figure 2 can then be converted to a change-in-mass versus charge plot (not shown) where the passed charge q is obtained by integrating the corresponding voltammogram. From the slope of the plot, the apparent mass of the species taken up is ∼10 amu. Experiments with other films yielded values ranging from 5 to 10 amu, suggesting the simultaneous uptake of H^+ and H_3O^+. A second EQCM experiment in D_2O, however, yielded Δf versus E (Figure 2) and Δf versus q plots having almost twice the slopes of corresponding plots obtained in H_2O. The isotope experiments unambiguously establish the species as exclusively H^+ and D^+. The origin of the falsely high-mass response from eq 1 is unclear but appears to be film thickness dependent. Conceivably the effect is associated in some way with the high porosity of the semiconductor film.

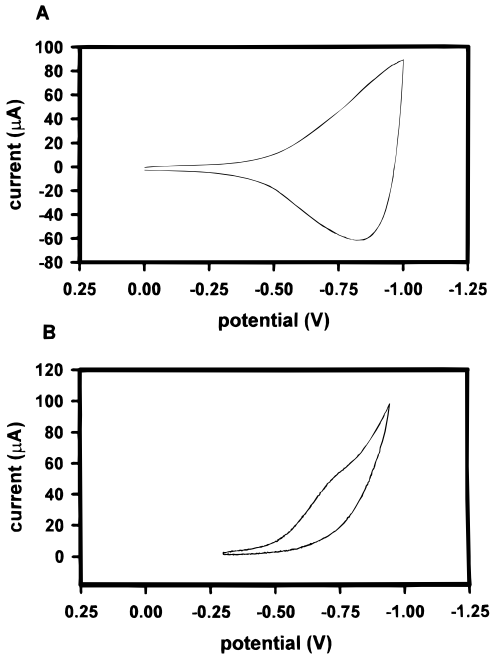

Figure 3. Cyclic voltammetry of nanocrystalline ZnO films at pH 8 on substrates consisting of (a) ITO and (b) gold QCM oscillator electrode. Scan rates: ITO = 100 mV/s, gold = 50 mV/s.

Similar EQCM responses were obtained at pH 5, but with a positively shifted onset potential (as expected from the general dependence of E_{CB} on pH for metal oxide semiconductors[13]). Returning to the experiments at pH 10, we note that the concentration of free protons or hydronium ions is necessarily vanishingly small. It follows that the source of protons, at least in high-basicity environments, is the solvent.

Zinc Oxide. Related experiments were pursued with films comprised of nanocrystalline zinc oxide. Following Weller,[3] we observed reversible, symmetrical cyclic voltammetry from films prepared on flat ITO surfaces (see Figure 3A). The onset potential for nonfaradaic current flow again can be identified as approximately E_{CB}. Nominally the same preparation on gold surfaces (coated QCM crystals) yielded much less well-defined, and much less reversible, voltammograms (Figure 3B). The differences are tentatively attributed to differences in semiconductor film thickness and effective area, with the irreversibility in Figure 3B arising from electroreduction of residual dissolved oxygen.

EQCM measurements with zinc oxide electrodes proved much more difficult than measurements with tin oxide because of the inherent chemical reactivity of ZnO. For example, at pH 4 we observed large, spontaneous (open circuit) mass changes due to rapid corrosion of ZnO. Better open-circuit stability was encountered at pH 8. Nevertheless, significant problems with chemical irreversibility and film degradation (dissolution and/or Zn^{2+} migration and electroreduction) were again encountered once electrode potentials were taken negative of E_{CB} (ca. −0.7 V at pH 8). Consequently, stable EQCM signals could be recorded for only a few (typically less than 10) voltammetric scans.

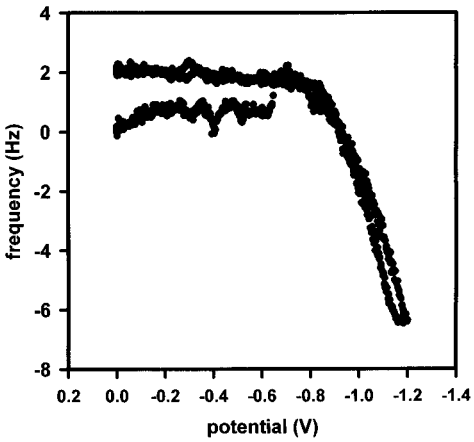

Figure 4. Oscillator frequency versus potential plot for nanocrystalline zinc oxide illustrating mass uptake at potentials negative of E_{CB}. Scan rate = 50 mV/s.

Figure 4 shows a representative "early" EQCM scan. Despite the film stability problem, the experiment clearly shows that mass increase (cation uptake) occurs at potentials more negative than E_{CB} (i.e., potentials where reversible electron addition can occur). We assume that the species responsible for the mass increase is again H^+. Nevertheless, attempts to confirm the assumption were inconclusive. Several experiments yielded roughly 2:1 D_2O:H_2O frequency change versus potential (or charge) responses; several others, however, did not. We assume that the lack of reproducibility is associated with film instability. (Note that successful implementation of the isotope experiment, for any given film, requires that film degradation be almost completely avoided over the course of successive light water/heavy water experiments.)

Discussion

Conventional descriptions of interfacial electron addition imply charge compensation via diffuse double-layer rearrangement on the solution side of the interface. For bulk semiconductor electrodes, the descriptions also imply space charge layer formation (electrical field creation) on the semiconductor side of the interface.[21] The EQCM results presented here lead to a new and qualitatively different description of interfacial energetics, at least for SnO_2/water and ZnO/water interfaces. For the former, the electron addition process can be written as

$$SnO_2 + e^-(\text{external}) + H^+(\text{solution}) \rightarrow SnO(OH)\cdot e^-_{CB} \quad (2)$$

Alternatively, a more localized description would be

$$Sn^{IV}O_2 + e^-(\text{external}) + H^+(\text{solution}) \rightarrow Sn^{III}O(OH) \quad (3)$$

In either case, interfacial electroneutrality is maintained by cation intercalation.

The ability of the material to achieve *local* electroneutrality via proton intercalation largely eliminates the need (under electron addition conditions) for compensating semiconductor space charge layer and electrolyte diffuse double-layer formation.[22] The absence of significant charge separation (note that the electron and proton are intimately associated in eqs 2 and 3) should also largely eliminate the internal electric potential gradient usually assumed for space charge layer formation. On the other hand, gradients in *chemical* potential should still exist for both the electron and proton since intercalation presumably is a near-surface phenomenon. In view of electron/proton mobility differences, however, the chemical potential gradient should still provide a basis for current flow, albeit via diffusion rather than migration.

Returning to the issue of electric potential gradients, the elimination of internal gradients implies that the potential instead must drop primarily across the *solution* side of the interface, as observed for metal electrode/solution interfaces. Expressed another way, eqs 2 and 3 imply that under what have often been termed (presumably incorrectly[1d]) accumulation conditions, the conduction band edge becomes unpinned—at least at potentials substantially negative of the nominal value for E_{CB}. Cao et al. have discussed related optical evidence for possible band edge unpinning at the TiO_2/water interface.[1d]

Equations 2 and 3 (and the corresponding expressions for zinc oxide) also suggest an interesting alternative explanation for the well-known dependence of E_{CB} for metal oxide semiconductors on pH (shifts of approximately −60 mV per pH unit). Standard explanations for energy shifts emphasize the role of open-circuit surface protonation where the resulting surface charge necessarily induces a potential perturbation. We intend to discuss the "standard" explanation and possible alternative explanations in more detail elsewhere. Briefly, however, two criticisms of the former can be made. First, if comparisons are made over a wide pH range, changes in E_{CB} can greatly exceed adsorption-induced changes in the ζ potential. Secondly, for closely related nanocrystalline titanium dioxide electrodes, Nernstian energy shifts are observable even in acidic solutions that are extremely far removed from the pH of zero charge (i.e., pH's where ζ potentials are invariant and all available, reactive surface oxo groups have already been protonated).[23] On the other hand, the 1:1 electron:proton stoichiometric ratio and the redox or quasi-redox character of eqs 2 and 3 lead, in a straightforward fashion, to a predicted −59 mV/pH unit shift in E_{CB}. To expand briefly, the product state in either eq 2 or 3 is a material of fixed H^+ content or activity. The reactants include one component, H^+(solution), of obviously variable activity. Because the conversion from reactants to product entails electron accumulation, transport or uptake, the corresponding potential (E_{CB}) is expected to vary as $(RT/F)\log\{1/a_{H+(\text{solution})}\}$. We note that this Pourbaix-type interpretation, while unconventional for *photo*electrode materials, is, in fact, the preferred interpretation for the electrochemistry of a number of other electrode materials, including oxides of ruthenium,[24] iridium,[25] manganese,[26] tungsten,[27] and vanadium.[28]

Finally, the coupled electron/proton nature of the interface energetics raises interesting questions concerning the appropriate energetics for electron transfer (ET) steps in isolation. Examples would include fast ET to and from surface-bound dye molecules. At least one recent report has suggested, based on kinetics measurements, that the dye formal potential/E_{CB} energy difference may not be the correct parameter for characterization of the isolated energetics of metal oxide semiconductor (in this case, titanium dioxide) to dye electron transfer processes.[29] In light of the present experiments, we hope to examine the electron transfer question for tin oxide electrodes.

Conclusions

EQCM measurements provide compelling evidence for charge-compensating cation uptake by nanocrystalline SnO_2 and ZnO electrodes during electron addition. Solvent isotope studies show conclusively for tin oxide (but less conclusively for ZnO) that the cation taken up is the proton. Additional studies as a function of solution pH implicate water, rather than hydronium ion, as the proton source. The new results, when combined

with previous results for titanium dioxide in nonaqueous electrolytes, suggest that charge-compensating cation intercalation may well represent a general mode of reactivity for metal oxide semiconductors. Finally, the new observations raise interesting fundamental questions regarding (1) chemical control of band energetics, (2) possible band edge unpinning phenomena, and (3) relationships between band edge energies and driving forces for isolated electron transfer reactions.

Acknowledgment. We thank the Office of Naval Research and the DOD AASERT program for support of our research. J.T.H. also gratefully acknowledges unrestricted support from the Dreyfus Foundation (Teacher-Scholar Award, 1991−96).

References and Notes

(1) For representative studies of TiO_2, see: (a) Rothenberger, G.; Fitzmaurice, D.; Grätzel, M. *J. Phys. Chem.* **1992**, *96*, 5983. (b) Redmond, G.; Fitzmaurice, D. *J. Phys. Chem.* **1993**, *97*, 1426. (c) Basame, S. B.; White, H. S. *J. Phys. Chem.* **1995**, *99*, 16430. (d) Cao, F.; Oskam, G.; Searson, P. C.; Stipkala, J. M.; Heimer, T. A.; Farzad, F.; Meyer, G. M. *J. Phys. Chem.* **1995**, *99*, 11974. (e) Enright, B.; Redmond, G.; Fitzmaurice, D. *J. Phys. Chem.* **1994**, *98*, 6195.

(2) For representative studies of SnO_2, see: (a) Nas, R.; Kamat, P. V. *Langmuir* **1995**, *11*, 1777. (b) Liu, K.; Kamat, P. V. *J. Electrochem. Soc.* **1995**, *142*, 835.

(3) For representative studies of ZnO, see: (a) Hoyer, P.; Weller, H. *J. Phys. Chem.* **1995**, *99*, 14096. (b) Hoyer, B.; Eichberger, R.; Weller, H. *Ber. Bunsen-Ges. Phys. Chem.* **1993**, *97*, 630.

(4) For reviews, see: (a) Hagfeldt, A.; Gratzel, M.; *Chem. Rev.* **1995**, *95*, 49. (b) Weller, H.; Eychmuller, A. *Adv. Photochem.* **1995**, *20*, 165.

(5) For example, see: (a) Kavan, L.; O'Regan, B.; Kay, A.; Grätzel, M. *J. Electroanal. Chem.* **1993**, *346*, 291. (b) Hotchandani, S.; Kamat, P. V. *J. Electrochem. Soc.* **1992**, *139*, 1630.

(6) For representative work, see: (a) Kormann, C.; Bahnemann, D. W.; Hoffmann, M. R. *J. Phys. Chem.* **1988**, *92*, 5196. (b) Koch, U.; Fojtik, A.; Weller, H.; Henglein, A. *Chem. Phys. Lett.* **1985**, *122*, 507.

(7) We recognize that apparent valence band and conduction band reactivity could also correspond to reactivity from shallow traps or from otherwise localized holes or electrons.

(8) For a recent review, see: Rajeshwar, K. *J. Appl. Electrochem.* **1995**, *25*, 1067.

(9) (a) Wang, C. M.; Mir, Q.-C.; Malekania, S.; Mallouk, T. E. *J. Am. Chem. Soc.* **1988**, *110*, 3710. (b) Wang, C. M.; Mallouk, T. E. *J. Phys. Chem.* **1990**, *94*, 423.

(10) For example, see: Bard, A. J. *J. Phys. Chem.* **1982**, *86*, 172.

(11) For reviews, see: (a) Meyer, G. J.; Searson, P. C. *Interface* **1993**, *33*, 115. (b) Grätzel, M. *Coord. Chem. Rev.* **1991**, *111*, 167. (c) Kamat, P. V. *Chem. Rev.* **1993**, *93*, 267.

(12) (a) Lu, H.; Preiskorn, J. N.; Hupp, J. T. *J. Am. Chem. Soc.* **1993**, *115*, 4927. (b) Yan, S. G.; Hupp, J. T. *J. Phys. Chem.* **1996**, *100*, 6867. (c) Moser, J.; Grätzel, M. *Chem. Phys.* **1993**, *176*, 493. (d) Ford, W. E.; Rodgers, M. A. J. *J. Phys. Chem.* **1994**, *98*, 3822. (e) Fessenden, R. W.; Kamat, P. V. *J. Phys. Chem.* **1995**, *99*, 12902. (f) Eichberger, R.; Willig, F. *Chem. Phys.* **1990**, *141*, 159.

(13) Bolts, J. M.; Wrighton, M. S. *J. Phys. Chem.* **1976**, *80*, 2641.

(14) For ideal semiconductor/solution interfaces, currents (albeit typically small currents) can also flow under conditions of weak depletion.

(15) Bejda, I.; Hotchandani, S.; Kamat, P. V. *J. Phys. Chem.* **1993**, *97*, 11064.

(16) Lyon, L. A.; Hupp, J. T. *J. Phys. Chem.* **1995**, *99*, 15718.

(17) See also: (a) Hagfeldt, A.; Vlachopoulos, N.; Grätzel, M. *J. Electrochem. Soc.* **1994**, *141*, L82. (b) Kavan, L.; Kratochvilová, K.; Grätzel, M. *J. Electroanal. Chem.* **1995**, *394*, 93.

(18) Spanhel, L.; Anderson, M. A. *J. Am. Chem. Soc.* **1991**, *113*, 2826.

(19) (a) Bejda, I.; Hotchandani, S; Kamat, P. V. *J. Phys. Chem.* **1994**, *98*, 4133. (b) Redmond, G.; O'Keefe, A.; Burgess,C.; MacHale, C.; Fitzmaurice, D. *J. Phys. Chem.* **1993**, *97*, 11081.

(20) Sauerbrey, G. *Z. Phys.* **1959**, *155*, 206.

(21) For example, see: Morrison, S. R. *The Chemical Physics of Semiconductor Surfaces*; Plenum Press: New York, 1977.

(22) On the other hand, the description does allow for space charge layer formation under *depletion* conditions. Compelling optical evidence for depletion-based space charge layer creation within bulk titanium dioxide electrodes has recently been reported by Lantz, Baba, and Corn (*J. Phys. Chem.* **1993**, *97*, 7392).

(23) Lemon, B. I.; Lyon. L. A., unpublished experimental data.

(24) Mitchell, D.; Rand, D. A. J.; Woods, R. *J. Electroanal. Chem.* **1978**, *89*, 11.

(25) (a) Pickup, P. G.; Birss, V. I. *J. Electroanal. Chem.* **1988**, *240*, 185. (b) Burke, L. D.; Whelan, D. P. *J. Electroanal. Chem.* **1984**, *121*, 121. (c) Johnson, C. S.; Hupp, J. T. *J. Electroanal. Chem.* **1993**, *345*, 351.

(26) Burke, L. D.; Murphy, O. J. *J. Electroanal. Chem.* **1980**, *109*, 373.

(27) Natan, M. J.; Wrighton, M. S. *J. Phys. Chem.* **1987**, *91*, 648.

(28) Burke, L. D.; O'Sullivan, E. J. M. *J. Electroanal. Chem.* **1980**, *111*, 383.

(29) Yan, S. G.; Hupp, J. T. *J. Phys. Chem.* **1996**, *100*, 6867.